Clinical Cancer Research

DS-8201a, A Novel HER2-Targeting ADC with a Novel DNA Topoisomerase I Inhibitor, Demonstrates a Promising Antitumor Efficacy with Differentiation from T-DM1

Yusuke Ogitani[1], Tetsuo Aida[1], Katsunobu Hagihara[1], Junko Yamaguchi[1], Chiaki Ishii[1], Naoya Harada[1], Masako Soma[1], Hiromi Okamoto[1], Masataka Oitate[1], Shingo Arakawa[1], Takehiro Hirai[2], Ryo Atsumi[1], Takashi Nakada[1], Ichiro Hayakawa[1], Yuki Abe[1], and Toshinori Agatsuma[1]

Abstract

Purpose: An anti-HER2 antibody–drug conjugate with a novel topoisomerase I inhibitor, DS-8201a, was generated as a new antitumor drug candidate, and its preclinical pharmacologic profile was assessed.

Experimental Design: *In vitro* and *in vivo* pharmacologic activities of DS-8201a were evaluated and compared with T-DM1 in several HER2-positive cell lines and patient-derived xenograft (PDX) models. The mechanism of action for the efficacy was also evaluated. Pharmacokinetics in cynomolgus monkeys and the safety profiles in rats and cynomolgus monkeys were assessed.

Results: DS-8201a exhibited a HER2 expression-dependent cell growth–inhibitory activity and induced tumor regression with a single dosing at more than 1 mg/kg in a HER2-positive gastric cancer NCI-N87 model. Binding activity to HER2 and ADCC activity of DS-8201a were comparable with unconjugated anti-HER2 antibody. DS-8201a also showed an inhibitory activity to Akt phosphorylation. DS-8201a induced phosphorylation of Chk1 and Histone H2A.X, the markers of DNA damage. Pharmacokinetics and safety profiles of DS-8201a were favorable and the highest non-severely toxic dose was 30 mg/kg in cynomolgus monkeys, supporting DS-8201a as being well tolerated in humans. DS-8201a was effective in a T-DM1–insensitive PDX model with high HER2 expression. DS-8201a, but not T-DM1, demonstrated antitumor efficacy against several breast cancer PDX models with low HER2 expression.

Conclusions: DS-8201a exhibited a potent antitumor activity in a broad selection of HER2-positive models and favorable pharmacokinetics and safety profiles. The results demonstrate that DS-8201a will be a valuable therapy with a great potential to respond to T-DM1–insensitive HER2-positive cancers and low HER2–expressing cancers. *Clin Cancer Res; 22(20); 5097–108. ©2016 AACR.*

Introduction

HER2 is a member of the EGFR family of transmembrane receptors (1) and overexpresses in a broad number of cancer types, such as bladder, breast, cervical, cholangio, colorectal, endometrial, esophageal, gastric, head and neck, liver, lung, ovarian, and salivary gland cancers (2, 3). Especially, amplification and overexpression of HER2 occurs in 25% to 30% of the instances of human breast cancer and are associated with a poor prognosis (4, 5). Several HER2-targeting therapies such as trastuzumab (6, 7), lapatinib (8), pertuzumab (9), and T-DM1 (10) have been approved worldwide for patients with HER2-positive tumors, which are defined as either IHC 3+ or IHC 2+/FISH–positive. However, there is no HER2-targeting therapy targeting HER2-weak–positive tumors such as IHC 2+/FISH-negative and IHC 1+.

Among the HER2-targeting drugs, T-DM1 is the only antibody–drug conjugate (ADC) in the market which is composed of trastuzumab and a tubulin polymerization inhibitor, DM1 (11). In its phase III clinical trial, EMILIA study, T-DM1 was shown to prolong survival and improve quality of life in a well-balanced manner with higher levels of efficacy and safety in HER2-positive breast cancer patients (10).

Other than T-DM1, SGN-35 (Brentuximab vedotin) has been approved (12) and more than 30 kinds of ADC programs are currently in clinical trials (13). However, most of them are applied to linker-payload systems similar to T-DM1 or SGN-35 (Brentuximab vedotin), which carry tubulin polymerization inhibitors (DM1 and MMAE, respectively). In the clinical trials of these tubulin inhibitor–conjugated ADCs, several dose-limiting toxicities such as thrombocytopenia, neutropenia, and neuropathy were observed, and some were considered to be mediated by the free drugs in plasma (14). Considering these situations, an improvement of linker-payload systems in terms of different antitumor spectrum, overcoming drug resistance to the

[1]Daiichi Sankyo Co., Ltd., Tokyo, Japan. [2]Clinical Development Department, Daiichi Sankyo RD Novare Co., Ltd., Tokyo, Japan.

Note: Supplementary data for this article are available at Clinical Cancer Research Online (http://clincancerres.aacrjournals.org/).

Corresponding Author: Yusuke Ogitani, Daiichi Sankyo Co., Ltd., 1-2-58, Hiromachi, Shinagawa-ku, Tokyo, 140-8710, Japan. Phone: 813-3492-3131; Fax: 813-5740-3641; E-mail: ogitani.yusuke.ds@daiichisankyo.co.jp

doi: 10.1158/1078-0432.CCR-15-2822

Translational Relevance

Most of the antibody–drug conjugates (ADC) in the market and in clinical trials are conjugated with the same type of drug, tubulin polymerization inhibitor. Currently, the development of a new drug linker system focusing on different types of drugs has been progressing. DS-8201a is a HER2-targeting ADC structurally composed of a humanized anti-HER2 antibody, enzymatically cleavable peptide linker, and a novel topoisomerase I inhibitor. DS-8201a showed potent antitumor activity based on the combination of pharmacologic effects of the antibody component with topoisomerase I inhibition. The stability in plasma was favorable and the safety profiles in rats and cynomolgus monkeys were acceptable into clinical trials. Moreover, DS-8201a was effective against T-DM1–insensitive tumors and HER2 low-expressing tumors. These data suggest that DS-8201a has the potential to respond to not only T-DM1–refractory breast cancer and HER2-positive patients, but IHC 1+ and 2+/FISH–negative patients for whom current HER2-targeting therapies are ineffective.

conventional systems, and providing a greater safety profile would be much desired.

Using our original linker-payload technology, we have designed DS-8201a, a new HER2-targeting ADC composed of a humanized anti-HER2 antibody, enzymatically cleavable peptide-linker, and a novel topoisomerase I inhibitor. Topoisomerase I inhibitors such as irinotecan (CPT-11) bind to topoisomerase I-DNA cleavable complexes and stabilize them, resulting in the induction of double-strand DNA breaks and apoptosis (15). In a clinical setting, these are widely used for colorectal (16), gastric (17), and other cancers (18–21). We previously developed exatecan mesylate (DX-8951f) as a novel topoisomerase I inhibitor which had more potent efficacy than CPT-11 against various tumor xenograft models, including CPT-11–resistant tumors *in vivo* (22), and a phase III trial in pancreatic cancer was conducted (23). A DX-8951 derivative (DXd) was used as the conjugated drug for DS-8201a, aiming to provide an additional and promising pharmacologic option for current HER2-targeting therapy.

In addition, our linker-payload system enabled conjugation with 8 molecules of DXd per antibody. The drug-to-antibody ratio (DAR) of current ADCs ranges from 2 to 4 as a higher DAR could have some problems, including fast clearance of the ADC *in vivo*, and a higher exposure to the released drug in plasma associated with off-target toxicities (24). In the case of T-DM1, systemic clearance of T-DM1 was more rapid than clearance of total trastuzumab in both cynomolgus monkeys and humans, and released DM1 was detectable (25, 26). DS-8201a is a stable and homogeneous DAR 8 ADC without the drawbacks above and is expected to steadily deliver much of the potent topoisomerase I inhibitor to the tumors.

Herein, we describe the preclinical profile of DS-8201a, including efficacy, pharmacokinetics, and safety. DS-8201a showed excellent antitumor activity against a T-DM1–insensitive model and HER2-low expression models, and a favorable pharmacokinetics and safety profile, suggesting its potential to address unmet medical needs in HER2-expressing patients.

Materials and Methods

Antibodies and ADCs

The anti-HER2 Ab was a human monoclonal IgG1 produced with reference to the same amino acid sequence as trastuzumab, and DS-8201a was synthesized according to the conjugation procedure described in another report (27) using the anti-HER2 Ab; its DAR was 7.7, as determined by reverse-phase chromatography (RPC). The drug distribution was analyzed by hydrophobic interaction chromatography (HIC). T-DM1 was purchased from Genentech or synthesized according to a previous report (28). Human IgG1 was purchased from Eureka Therapeutics Inc. Control IgG-ADC was synthesized using the same method as DS-8201a, resulting in a comparable DAR. Anti-HER2 ADC with DAR 3.4 was synthesized with a similar method to that of DS-8201a.

Cell lines

The human gastric carcinoma cell line NCI-N87, the human breast adenocarcinoma cell lines SK-BR-3 and MDA-MB-468, and the human pancreatic cancer cell lines Capan-1 and CFPAC-1 were purchased from ATCC. The human breast cancer cell line JIMT-1 was purchased from DSMZ. The human breast cancer cell line KPL-4 was provided from Dr. Kurebayashi at the Kawasaki Medical University (Okayama, Japan). The human gastric cancer cell line GCIY was provided by the Institute of Physical and Chemical Research (Japan). All cell lines except for MDA-MB-468 were cultured with appropriate mediums (RPMI1640 medium for KPL-4, NCI-N87, and GCIY, McCoy 5A Medium for SK-BR-3, DMEM for JIMT-1, and IMDM for Capan-1 and CFPAC-1) supplemented with 10% heat-inactivated FBS at 37°C and 5% CO_2 atmosphere. MDA-MB-468 was cultured with Leibovitz's L-15 medium supplemented with 10% heat-inactivated FBS at 37°C in a free gas exchange with atmospheric air.

Topoisomerase I inhibitory assay

SN-38 was purchased from Tokyo Chemical Industry Co., Ltd. and DX-8951f and DX-8951 derivative (DXd) was synthesized in-house. The inhibitory activities of SN-38, DX-8951f, and DXd against human topoisomerase I were evaluated by a topoisomerase I–mediated DNA relaxation assay according to a previous report (29). Briefly, recombinant human topoisomerase I was incubated with each drug for 5 minutes. Then, supercoiled DNA pBR322 was added and incubated at 25°C for 60 minutes. After the electrophoresis of the mixture on an agarose gel, the amount of the supercoiled DNA was measured with a CCD imager.

Cytotoxic assay

Cells were seeded to a 96-well plate at 1,000 cells per well. After overnight incubation, each diluted substance was added. Cell viability was evaluated after 6 days using a CellTiter-Glo Luminescent Cell Viability Assay from Promega Corp. according to the manufacturer's instructions. For the detection of HER2 expression in each cell line, cells were incubated on ice for 30 minutes with FITC Mouse IgG1, κ Isotype Control, or anti-HER2/neu FITC from Becton, Dickinson and Company. After washing, the labeled cells were analyzed by FACSCalibur (Becton, Dickinson and Company). Relative mean fluorescence intensity (rMFI) was calculated by the following equation:

$$\frac{\text{MFI of anti-HER2 Ab-FITC}}{\text{MFI of isotype control-FITC}}$$

Cell line and patient-derived xenograft studies

All *in vivo* studies were performed in accordance with the local guidelines of the Institutional Animal Care and Use Committee. Detailed study procedures are written in the supplement. Briefly, each cell suspension or tumor fragment was inoculated subcutaneously into specific pathogen-free female nude mice. When the tumor had grown to an appropriate volume, the tumor-bearing mice were randomized into treatment and control groups based on the tumor volumes, and dosing was initiated on day 0. Each substance was administered intravenously to the mice. Tumor growth inhibition (TGI, %) was calculated according to the following equation:

$$100 \times \frac{\text{Average tumor volume of the treated group}}{\text{Average tumor volume of the control group}}$$

Pharmacokinetics of DS-8201a in cynomolgus monkeys

Concentrations of DS-8201a and the total antibody in plasma were determined with a validated ligand-binding assay; the lower limit of quantitation was 0.100 μg/mL. Concentrations of DXd in plasma were determined with a validated liquid chromatography-tandem mass spectrometry (LC/MS-MS) method; the lower limit of quantitation was 0.100 ng/mL. DS-8201a was intravenously administered at 3.0 mg/kg to male cynomolgus monkeys. Plasma concentrations of DS-8201a, total antibody, and DXd were measured up to 672 hours postdose.

In vitro stability of DS-8201a in plasma

The release rate of DXd from DS-8201a at the concentration of 10 μg/mL at 37°C up to 21 days was evaluated in mouse, rat, monkey, and human plasma.

ELISA

For a binding assay, immunoplates were coated with 2.5 μg/mL His-tagged HER2-ECD protein (Sino Biological Inc.) in coating buffer and kept overnight at 4°C. After washing, the plates were blocked and each serially diluted substance was added to the wells. After incubation for 1.5 hours at 37°C, the plates were washed and incubated with HRP-conjugated anti-human IgG secondary antibody for 1 hour at 37°C. After washing, TMB solution was added and A_{450} in each well was measured with a microplate reader. For the detection of phosphorylated Akt (pAkt), SK-BR-3 cells were preincubated in a 96-well plate for 4 days and then incubated with each substance for 24 hours. After incubation, the cells were lysed and intercellular pAkt and total Akt were detected by using a PathScan Phospho-Akt1 (Ser473) Sandwich ELISA Kit and PathScan Total-Akt1 Sandwich ELISA Kit (Cell Signaling Technology, Inc.) according to the manufacturer's instructions. Relative pAkt of each sample well was calculated by dividing treated normalized pAkt values by untreated normalized pAkt values.

ADCC evaluation

Antibody-dependent cell-mediated cytotoxicity (ADCC) activities were evaluated using human peripheral blood mononuclear cells (PBMC) derived from a donor as effector cells and the SK-BR-3 cells as target cells. The effector cells (2×10^5 cells) and the ^{51}Cr-labeled target cells (1×10^4 cells) were incubated with each substance, and the indicating effector:target (E:T) ratio was 20:1. After 4 hours of incubation, ADCC activity was measured by radioactivity in the culture supernatant.

Immunoblotting

KPL-4 cells were treated with each substance. After 24, 48, or 72 hours, the cells were harvested and lysed with M-PER lysis buffer containing Halt Protease & Phosphatase Inhibitor Cocktail (Thermo Fisher Scientific Inc.).

The samples were loaded and separated by SDS-PAGE and blotted onto polyvinylidene difluoride membranes. The membranes were blocked, and probed overnight with anti-phospho-Chk1 (Ser345; 133D3) rabbit mAb, anti-Chk1 (2G1D5) mouse mAb, anti-cleaved PARP (Asp214) antibody, anti-β-actin (8H10D10) Mouse mAb (Cell Signaling Technology, Inc.), anti-phospho-Histone H2A.X (Ser139) antibody (Millipore), and anti-Histone H2A.X antibody (Abcam Plc.) at 4°C. Then, the membranes were washed and incubated with fluorescence-labeled secondary antibodies for 10 minutes using SNAP intradermally (Millipore). The fluorescence signal was detected using an Odyssey imaging system (LI-COR, Inc.).

Toxicity studies in rats and monkeys

DS-8201a was intravenously administered intermittently at 3-week intervals over a 6-week period to Crl:CD(SD) rats or cynomolgus monkeys (Table 1). Clinical signs, body weight, food consumption, and clinical pathology were monitored throughout the study. A necropsy was conducted on the day after the last administration. The reversibility of the toxic changes was assessed in a subsequent 9-week recovery period in rats and in a subsequent 6-week recovery period in cynomolgus monkeys.

Statistical analysis

All statistical analysis except for toxicity studies was performed using SAS System Release 9.1.3 and 9.2 (SAS Institute Inc.). Statistical analysis in toxicity studies was performed using MUSCOT (Yukms Co., Ltd.) All IC_{50} and ED_{50} values were determined by a Sigmoid Emax model, and dose dependency was evaluated by a Spearman rank correlation coefficient hypothesis test.

Results

Structure of DS-8201a

The structure of DS-8201a is shown in Fig. 1A. DS-8201a is a HER2-targeting ADC and is composed of an anti-HER2 antibody and a derivative of DX-8951 (DXd), a topoisomerase I inhibitor, which are bound together by a maleimide glycyn-glycyn-phenylalanyn-glycyn (GGFG) peptide linker. The linker-payload is conjugated with the antibody via the cysteine residues after the interchain disulfide bounds are reduced with a reducing agent, tris (2-carboxyethyl) phosphine hydrochloride (TCEP HCl). As the tetrapeptide is decomposed by lysosomal enzymes such as cathepsins B and L which are highly expressed in tumor cells (30–34), it is supposed that DS-8201a is cleaved by lysosomal enzymes and releases DXd, which attacks target molecules specifically in tumor cells after it binds to HER2 receptors and is internalized in tumor cells. By using RPC, the DAR of DS-8201a was determined as approximately 8, which is the theoretical maximum drug loading number for conventional interchain cysteine conjugation. Therefore, homogeneous drug distribution was observed in the HIC chart

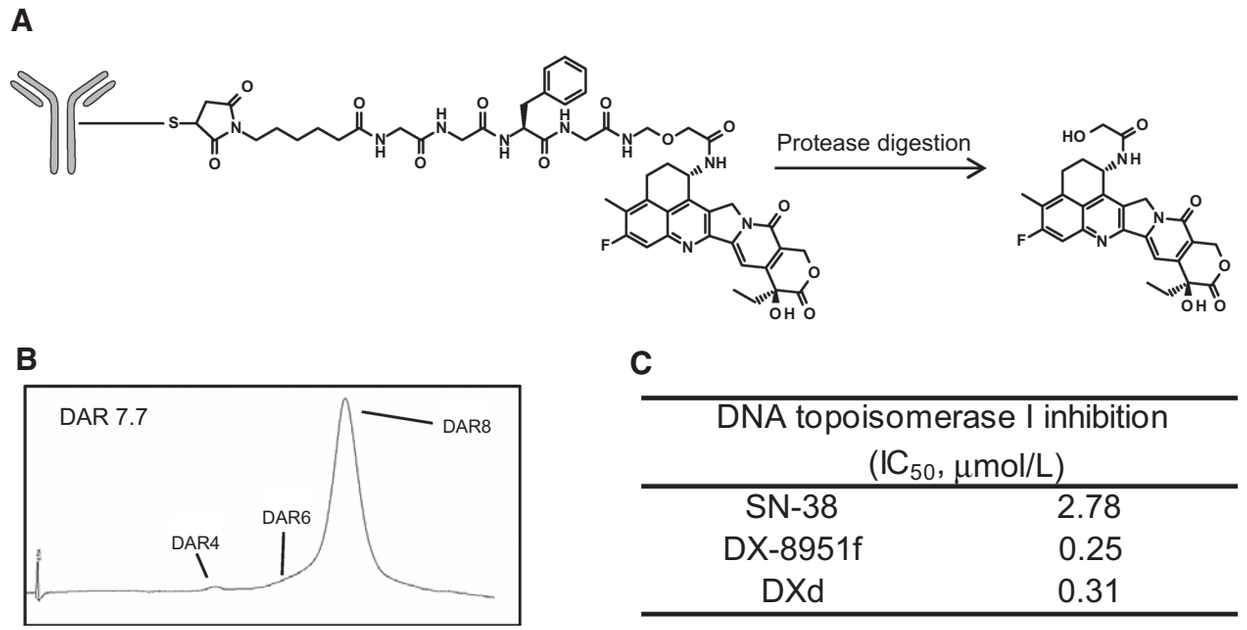

C

DNA topoisomerase I inhibition (IC_{50}, μmol/L)	
SN-38	2.78
DX-8951f	0.25
DXd	0.31

Figure 1.
Structure and characterization of DS-8201a. **A,** the chemical structure of the linkage of DS-8201a. **B,** the conjugated drug distribution by the reverse-phase chromatographic analysis. **C,** comparison of cell-free DNA topoisomerase I inhibitory activity among SN-38, DX-8951f and DXd. Each value represents the mean ($n = 2$ for SN-38 and DXd, $n = 8$ for DX-8951f).

(Fig. 1B). We confirmed that DXd is more potent in inhibitory activity in topoisomerase I than SN-38 as well as DX-8951f, as measured by a topoisomerase I–mediated DNA relaxation assay (Fig. 1C).

Inhibition of cancer cell growth by DS-8201a

The inhibitory activity of DS-8201a against cancer cell growth was compared with an anti-HER2 Ab and control IgG–ADC–conjugated with DXd against various human cancer cell lines *in vitro*. HER2 expression on the cell surface of the cell lines KPL-4, NCI-N87, SK-BR-3, and MDA-MB-468 was firstly evaluated by flow cytometric analysis (Fig. 2A). The relative MFIs of KPL-4, NCI-N87, and SK-BR-3 were 95.7, 101.6, and 56.2, respectively, suggesting that HER2 is clearly expressed on the cell surfaces, whereas the relative MFI was 1.0 for MDA-MB-468, indicating no expression in the MDA-MB-468. Remarkable inhibitory activity to the cell growth was observed for DS-8201a against HER2-positive KPL-4, NCI-N87, and SK-BR-3, with the IC_{50} values of 26.8, 25.4, and 6.7 ng/mL, respectively, whereas no such inhibition was seen against MDA-MB-468 with the IC_{50} value of >10,000 ng/mL (Fig. 2B). Although the anti-HER2 Ab showed cell growth–inhibitory activity against NCI-N87 and SK-BR-3, these activities were rather weaker than that of the DS-8201a; the IC_{50} values of NCI-N87 and SK-BR-3 were 204.2 and 65.9 ng/mL, respectively (Fig. 2B). Also, control IgG-ADC did not show cell growth–inhibitory activities in any of the four cell lines (Fig. 2B), although all four cell lines were sensitive to the payload, DXd (IC_{50}: 1.43 nmol/L–4.07 nmol/L). These results indicate that the cell growth–inhibitory activity of DS-8201a was remarkably enhanced by drug conjugation to the anti-HER2 Ab, and also that DS-8201a shows target-specific growth inhibition against HER2-positive cell lines.

Antitumor activity *in vivo*

The *in vivo* antitumor activity of DS-8201a was evaluated in a HER2-positive NCI-N87 xenograft model. DS-8201a induced tumor growth inhibition in a dose-dependent manner and tumor regression with a single dosing at more than 1 mg/kg without inducing any abnormalities in the general condition or body weight changes of the mice (Fig. 2C). In the same model, 4 mg/kg administration of anti-HER2 Ab partially inhibited the tumor growth, indicating 31% of tumor growth inhibition (TGI) compared with the control group on day 21 (Fig. 2D). On the other hand, DS-8201a clearly showed more potent antitumor efficacy, indicating 99% TGI at the same dose of 4 mg/kg, so that the enhancement of efficacy by drug conjugation was observed *in vivo* as well as in the *in vitro* models (Fig. 2D). Moreover, it is suggested that the *in vivo* efficacy of DS-8201a depends on its HER2 binding, as no inhibition of tumor growth was seen for the control-IgG ADC (Fig. 2D).

Pharmacokinetics in cynomolgus monkeys

The plasma DS-8201a concentrations decreased exponentially after a single intravenous administration of DS-8201a. The volume of distribution at steady state (V_{ss}) of DS-8201a and total antibody was close to the plasma volume (data not shown). No clear difference was observed in the pharmacokinetic profile between DS-8201a and the total antibody, indicating that the peptide-linker of DS-8201a is stable in plasma even at DAR 8 (Fig. 2E). A low level of DXd was detected only at the limited time points (Fig. 2E).

In vitro stability in plasma

The release rates of DXd from DS-8201a ranged from 1.2% to 3.9% on day 21 in mouse, rat, monkey, and human plasma (Fig.

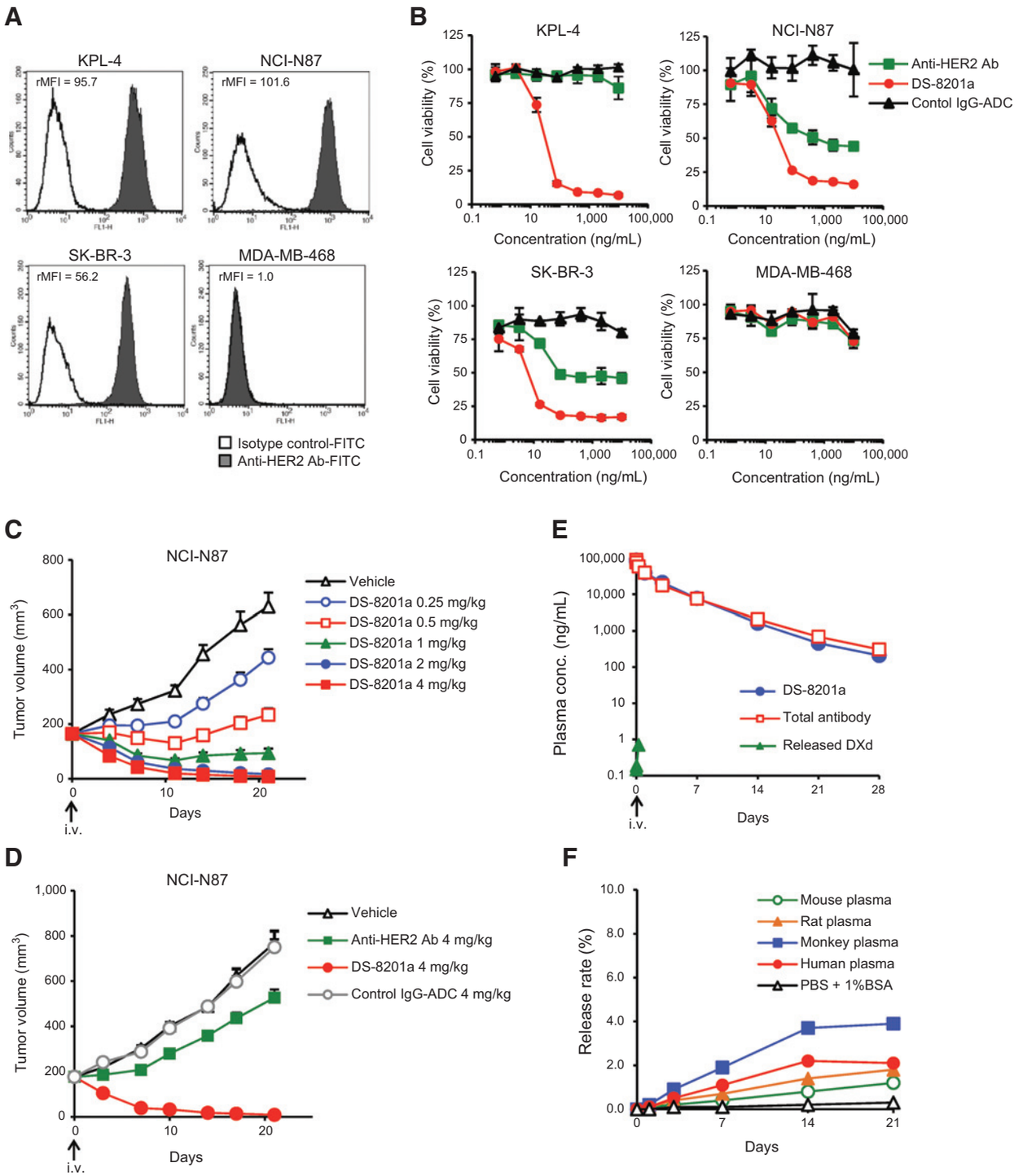

Figure 2.

In vitro and *in vivo* efficacy and stability in plasma of DS-8201a. **A,** HER2 expression in several cancer cell lines. **B,** *in vitro* cell growth inhibitory activity in the cell lines. The cells were treated with DS-8201a, anti-HER2 Ab, and control IgG-ADC for 6 days. Each point represents the mean and SD ($n = 3$). **C** and **D,** antitumor efficacy of DS-8201a in NCI-N87 xenograft model. The tumor-bearing mice were intravenously administered with DS-8201a, control IgG-ADC, and anti-HER2 Ab on day 0. Each point represents the mean tumor volume and SE ($n = 10$). **E,** pharmacokinetics of DS-8201a in cynomolgus monkeys. DS-8201a was intravenously administered to cynomolgus monkeys at the dose of 3 mg/kg ($n = 3$). **F,** *in vitro* stability of DS-8201a in plasma.

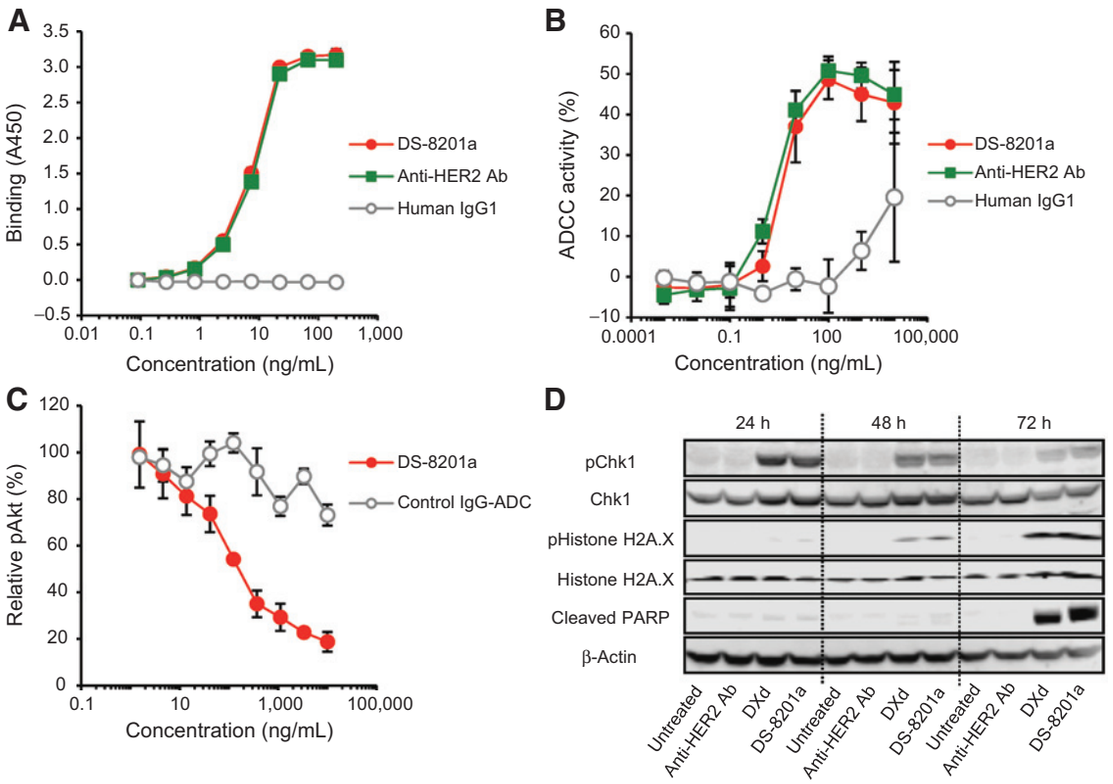

Figure 3.
Mechanisms of action of DS-8201a. **A,** binding to HER2 determined by ELISA. **B,** ADCC activity. Cr^{51}-labeled SK-BR-3 cells and PBMCs were mixed and incubated with each substance for 4 hours. Result of one of three donors is represented. **C,** inhibitory activity of pAkt phosphorylation. Intracellular pAkt levels in SK-BR-3 cells treated with DS-8201a and control IgG-ADC were measured by ELISA. **D,** induction of DNA damage and apoptosis. KPL-4 cells were treated with DS-8201a (10 μg/mL), anti-HER2 Ab (10 μg/mL), and DXd (10 nmol/L) for 72 hours. Several proteins were detected by Western blotting. Each point represents the mean and SD ($n = 3$).

2F), and these were comparable or rather lower than those of other ADCs, such as T-DM1, SGN-35 (Brentuximab vedotin), and inotuzumab ozogamicin (35–37). These results indicate that DS-8201a is stable in plasma.

Mechanism of action of DS-8201a

To confirm the effect of the drug conjugation with the anti-HER2 Ab on binding activity to HER2, K_d values of DS-8201a and the anti-HER2 Ab were determined by ELISA using HER2 ECD protein (Fig. 3A). K_d values were 7.3 ng/mL for DS-8201a and 7.8 ng/mL for the anti-HER2 Ab, indicating that drug conjugation did not affect HER2 binding. The major mechanisms of action of trastuzumab are thought to involve an ADCC activity by binding to FcγRIII on immune effector cells (38, 39), and a downregulation of phosphorylated Akt (pAkt), which upregulates p27 expression and inhibits cell proliferation (40). We investigated whether DS-8201a retains these same mechanisms of action as trastuzumab. Next, ADCC activity was measured by the detection of SK-BR-3 cell lysis mediated by human PBMCs. DS-8201a showed ADCC activity, resulting in 48.6% of maximum cytotoxicity with an EC_{50} of 3.8 ng/mL (Fig. 3B), and this effect was similar to the anti-HER2 Ab. Regarding the inhibition of phosphorylation of Akt, DS-8201a induced the downregulation of the intracellular pAkt (Ser473) in the SK-BR-3 cells in a dose-dependent manner after treatment for 24 hours (Fig. 3C). In the same condition, the control IgG ADC did not affect the pAkt status. In SK-BR-3 cells, the treatment of trastuzumab decreased about 70% of the Akt phosphorylation (41), suggesting that DXd conjugation may enhance the effect of unconjugated anti-HER2 antibody on pAkt. These evaluations of ADCC and pAkt indicate that DS-8201a retains the functions of trastuzumab after DXd conjugation.

On the other hand, DNA damage and apoptosis induced by topoisomerase I inhibition were evaluated by detecting phosphorylations of Chk1 and Histone H2A.X (the markers of DNA damage; refs. 42, 43), and cleaved PARP (the marker of apoptosis; ref. 44) in the KPL-4 cells in the presence of DS-8201a, the anti-HER2 Ab, or DXd using the Western blotting method (Fig. 3D). An amount of 10 μg/mL of DS-8201a induced the phosphorylations of Chk1 and Histone H2A.X, and PARP cleavage. DXd induced the same changes as DS-8201a. Conversely, 10 μg/mL of anti-HER2 Ab did not induce a change in any of the objective proteins at any time point, including the untreated group. These results indicate that DS-8201a induced DNA damage and apoptosis in the same manner as DXd, and suggests that these changes were caused by the topoisomerase I inhibition activity of the released DXd from DS-8201a.

Therefore, DS-8201a is considered to exhibit HER2-specific cell growth inhibition and antitumor activity via a novel mechanism of action that combined the pharmacologic

Table 1. Summary of repeated dose toxicity studies in rats and monkeys

Species	Crl:CD(SD) rats	Cynomolgus monkeys
Doses	0, 20, 60 and 197 mg/kg	0, 10, 30 and 78.8 mg/kg
Regimens	Intravenous, every 3 weeks	Intravenous, every 3 weeks
	Days 1, 22, 43 (3 times in total)	Days 1, 22, 43 (3 times in total)
No. of animals	10/sex/group (Main): all dose groups	3/sex/group (Main): all dose groups
	5/sex/group (Recovery): 60 and 197 mg/kg groups	2/sex/group (Recovery): 30 and 78.8 mg/kg groups
Lethal dose	>197 mg/kg	78.8 mg/kg (1 female died)
Body weight	≤60 mg/kg: normal	≤30 mg/kg: normal
	197 mg/kg: low body weight gain	78.8 mg/kg: decreased in 1 male and 1 female
Hematology	20 mg/kg: normal	≤30 mg/kg: normal
	≥60 mg/kg: decreased RBC and WBC parameters	78.8 mg/kg: decreased RBC parameters
Target organs and tissues	≥20 mg/kg: intestines, testis	≥10 mg/kg: intestines
	≥60 mg/kg: bone marrow, thymus, lymph node, skin, kidney, incisor	≥30 mg/kg: lung, skin, testis
		78.8 mg/kg: bone marrow, kidney
STD_{10}/HNSTD	STD_{10}: >197 mg/kg	HNSTD: 30 mg/kg

Abbreviations: RBC, red blood cell; WBC, white blood cell.

activities of an anti-HER2 antibody with those of the topoisomerase I inhibitor, DXd.

Safety profile of DS-8201a

A repeated intravenous dosing (every 3 weeks for 3 doses) study was conducted in cynomolgus monkeys, the cross-reactive species for DS-8201a, and in rats (antigen–non-binding species; Table 1). In the rat study, no deaths or life-threatening toxicities were found at dose levels up to 197 mg/kg, the maximum dose. Therefore, the severely toxic dose of 10% in animals (STD_{10}) was considered to be >197 mg/kg. In the monkey study, one female at the highest dose of 78.8 mg/kg was euthanized due to moribundity on day 26. The cause of the moribundity appeared to be the deteriorated condition of the animal, which included decreased body weight and food consumption, as well as bone marrow toxicity and intestinal toxicity. Microscopic findings in the intestines, bone marrow and lungs in the surviving monkeys are shown in Supplementary Table S1. Gastrointestinal toxicity and bone marrow toxicity are typical dose-limiting factors in the clinical use of topoisomerase I inhibitors. The effects of DS-8201a on the intestines were very slight, and severe changes were not pronounced in any animal at up to 78.8 mg/kg. The bone marrow toxicity was produced only at 78.8 mg/kg, and was accompanied by decreases in reticulocyte ratios. No abnormalities in leukocyte and erythrocyte counts were observed in monkeys at 10 and 30 mg/kg. The repeated dose of DS-8201a caused moderate pulmonary toxicity in monkeys at 78.8 mg/kg, and findings graded as slight or very slight after the 6-week recovery period at ≥30 mg/kg. On the basis of the mortality and severity of the findings above, the highest non-severely toxic dose (HNSTD) for monkeys was considered to be 30 mg/kg. DS-8201a was well tolerated at the doses up to 197 mg/kg in rats and 30 mg/kg in monkeys following the repeated administration corresponding to the clinical regimen, and the nonclinical safety profile was acceptable for entry into human trials.

Antitumor activity of DS-8201a in low HER2–expressing tumors

T-DM1 has been approved for HER2-positive metastatic breast cancer patients, defined as being HER2 IHC 3+ or IHC 2+/FISH–positive according to the current guidelines (45), and there are still clinical unmet needs in FISH-negative, HER2 1+ and 2+ populations for HER2-targeting therapies. Therefore, the antitumor activity of DS-8201a was evaluated in various mice xenograft models with different HER2 expression levels; KPL-4 (strong positive), JIMT-1 (moderate positive), Capan-1 (weak positive), and GCIY (negative) (Fig. 4A and B). Anti-HER2 ADC with the same drug-linker as DS-8201a and about half the DAR (DAR 3.4) was also evaluated to investigate the effect of DAR on antitumor activity. While T-DM1 was effective against only the KPL4 model, DS-8201a was effective against all HER2-positive models with KPL4, JIMT-1, and Capan-1. Both ADCs were not effective in the GCIY model. Anti-HER2 ADC (DAR 3.4) inhibited tumor growth against all HER2-positive models, and the efficacy was HER2 expression–dependent. A stronger efficacy was apparently observed for DS-8201a than anti-HER2 ADC (DAR 3.4) in the HER2 weak–positive Capan-1 model. These results suggest that the high DAR ADC, DS-8201a, enables the delivery of sufficient payload amounts into cancer cells, indicating cytotoxicity even with low HER2 levels. In case of HER2 strong –positive models, even a low DAR ADC is able to deliver a sufficient amount of payload for cell death. DS-8201a was effective in tumors with broader HER2 levels due to its high DAR, approximately 8. To confirm HER2-specificity of DS-8201a in a HER2 low–expressing model, a competitive inhibition study was performed in a HER2 low CFPAC-1 model (Fig. 4C). The efficacy of DS-8201a was cancelled by the prior treatment of the anti-HER2 Ab, and the control IgG-ADC did not inhibit tumor growth at a 3-fold higher dose than DS-8201a. From these results, the HER2 specificity of DS-8201a in a HER2 low–expressing model was confirmed.

Comparison with T-DM1 in PDX models

In addition to the cell line–based xenograft models, several PDX evaluations were performed to assess clinical benefits more precisely. In a gastric cancer PDX model, NIBIO G016, DS-8201a demonstrated potent antitumor activity with tumor regression, but T-DM1 did not (Fig. 5A). As the HER2 status in this model was IHC 3+/FISH+, it is supposed that this difference in antitumor efficacy between DS-8201a and T-DM1 is based on the different sensitivity of payload due to dissimilar mechanism of action of each payload. In breast cancer PDX models, although both DS-8201a and T-DM1 were effective in the HER2 IHC 2+/FISH–positive ST225 model, complete tumor regression was observed on day 21 in 3 of 5 mice treated with DS-8201a, not T-DM1 (Fig. 5B). Furthermore, DS-8201a showed an antitumor activity in HER2 low–expressing ST565 and ST313 models with HER2 IHC 1+/FISH–negative

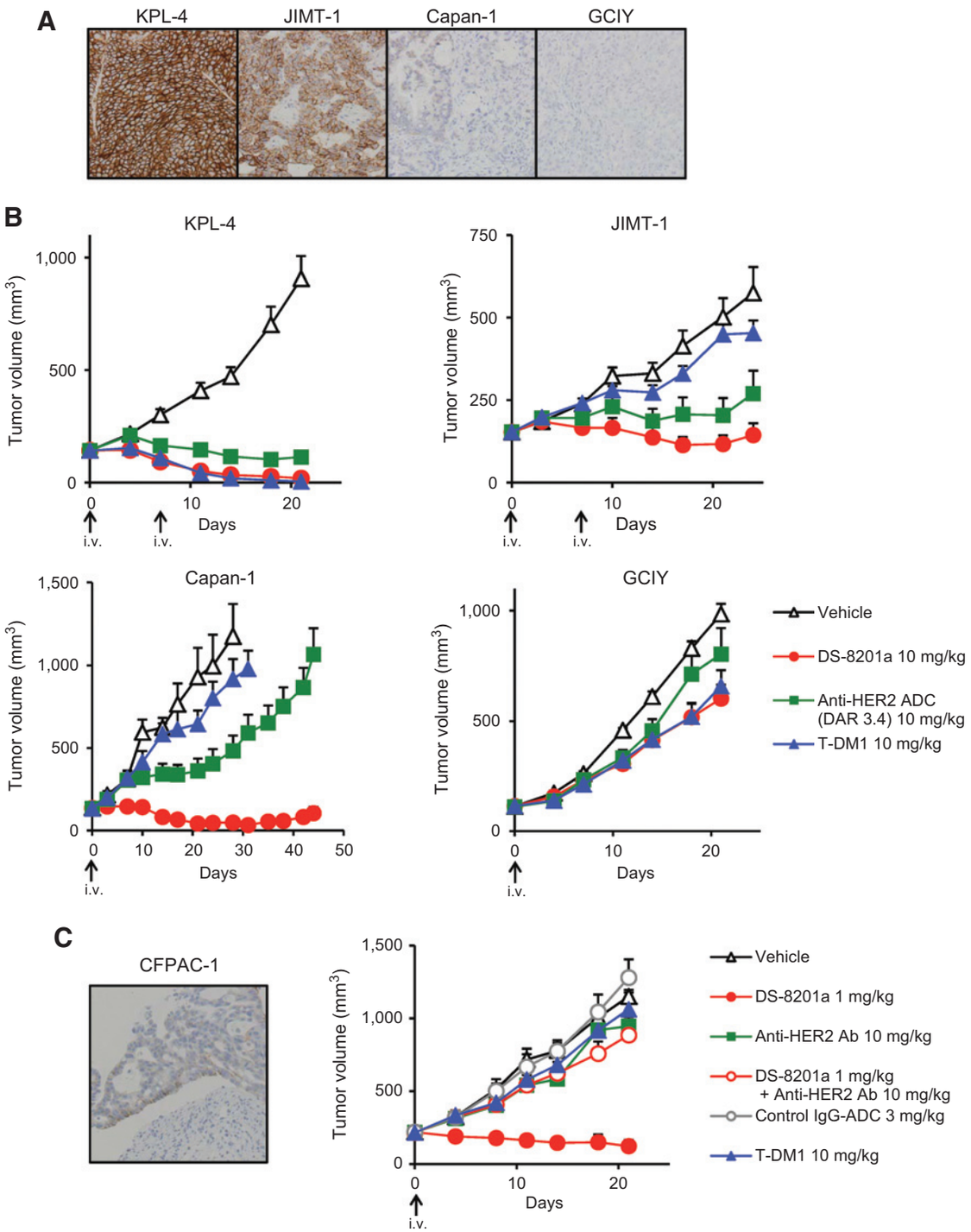

Figure 4.
Antitumor activity of DS-8201a against tumors with low HER2 level. **A,** HER2 IHC in several xenografted tumors. **B,** antitumor activity of DS-8201a compared with T-DM1 and anti-HER2 ADC (DAR 3.4). **C,** competitive study by anti-HER2 Ab against the efficacy of DS-8201a. Each point represents the mean and SE (n = 5–6).

expression (Fig. 5C and D), but T-DM1 did not. This result indicated a similar tendency to the cell line–based xenograft models such as Capan-1 and CFPAC-1 (Fig. 4B and C). Consequently, DS-8201a showed more potent antitumor activity than T-DM1 in all 4 of these models with several HER2 expression levels. These results suggest that DS-8201a has a differentiable potential from T-DM1, which shows effectiveness in T-DM1–insensitive and HER2 low–expressing tumors,

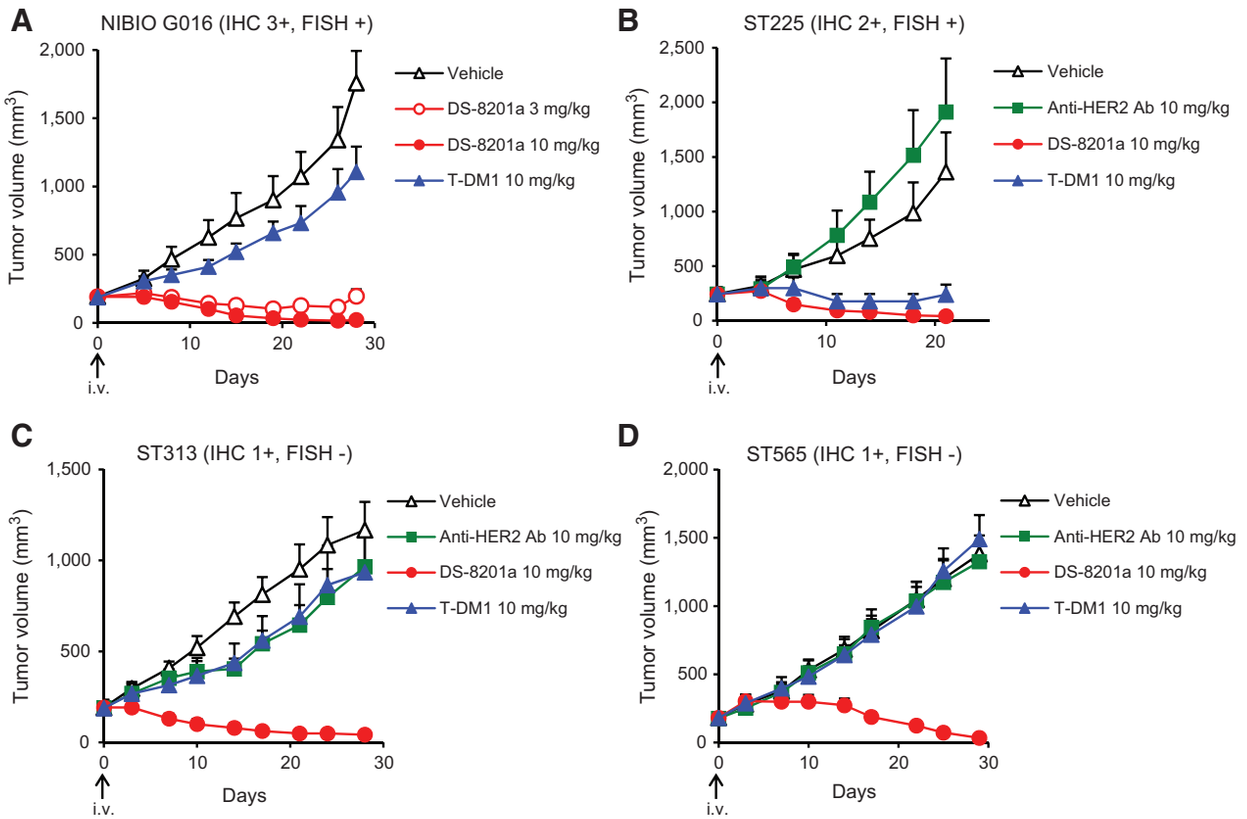

Figure 5.
The effect of DS-8201a compared with T-DM1 in several PDX models. **A,** gastric cancer PDX model with HER2 IHC 3+/FISH–positive. **B,** breast cancer PDX models with HER2 IHC 2+/FISH–positive. **C** and **D,** breast cancer PDX models with HER2 IHC 1+/FISH–negative. Each point represents the mean and SE ($n = 5$–6).

resulting from the different mechanisms of action of the conjugated drug and the high DAR of DS-8201a.

Discussion

Most of the ADCs currently in the market and in clinical development carry tubulin polymerization inhibitors such as T-DM1 and SGN-35 (Brentuximab vedotin; ref. 13). We synthesized a novel ADC with a topoisomerase I inhibitor, which has a different mechanism of action from tubulin polymerization inhibitors, and a novel self-immolative linker system using an aminomethylene (AM) moiety. Although other cleavable linker systems applied to SGN-35 (Brentuximab vedotin) and several ADCs release amino group–containing payloads, this AM self-immolative linker system is able to release DXd containing the hydroxyl group from DS-8201a. Moreover, this novel linker-payload system enables a reduction in the hydrophobicity of the ADC and helps increase its DAR. In the case of T-DM1, lysine conjugation and noncleavable systems are used, and it is quite a different system from DS-8201a. DS-8201a showed potent HER2-specific efficacy both *in vitro* and *in vivo*, and by drug conjugation maintained the functional effects of trastuzumab equal to those of T-DM1 (46). Furthermore, the safety profiles of DS-8201a in rats and cynomolgus monkeys showed DS-8201a as being well tolerated.

These favorable profiles are thought to be attributed to the high stability of DS-8201a in plasma, even as an ADC with DAR 8. ADCs with greater DAR (DAR 6 and 8) are generally unstable and show higher clearances, which can result in decreasing efficacy and increasing toxicity (24). In fact, in a mouse study, an anti-CD30 ADC conjugated with monomethyl auristatin E (MMAE) with DAR 8 did not improve the *in vivo* efficacy compared with the ADC with DAR 4 due to the accelerated plasma elimination of the ADC, and the therapeutic index was decreased 2-fold by the lowering of the MTD (24). Our newly developed drug linker system enabled the anti-HER2 ADC to be stable in plasma and have preferable pharmacokinetics regardless of its high DAR, exhibiting a potent *in vivo* antitumor activity dependent upon the increased DAR. In the pharmacokinetic/pharmacodynamic analysis of DS-8201a, the human pharmacokinetic profiles following repeated administration of DS-8201a every 3 weeks for 3 cycles were simulated using the monkey pharmacokinetic data. On the basis of the simulated C_{trough}, 0.8 mg/kg every 3 weeks of DS-8201a is expected to indicate some efficacy in the clinical setting (data not shown). The repeated dose monkey study with a every 3 weeks regimen revealed that DS-8201a caused no severe toxicities at up to 30 mg/kg (HNSTD), indicating a wide therapeutic window.

The achievement of the DAR 8 ADC synthesis contributed to the antitumor effect on tumors with a low HER2 level. DS-

8201a with DAR 8 showed potent antitumor activity in HER2 low–expressing models, though the anti-HER2 ADC with DAR 3.4 did not. As the efficacy in HER2 low–expressing models was observed in a HER2-dependent manner, it was suggested that DS-8201a enables the delivery of more DXd to HER2 low–expressing tumor cells than a lower DAR ADC. On the other hand, T-DM1 was not effective in these models, and the lower DAR of T-DM1 (DAR 3.5) than DS-8201a was considered to be one of the reasons. These results indicate the expansion of the patient population for DS-8201a treatment. Although HER2-positive patients who are defined as either IHC3+ or IHC2+/FISH–positive are treated with current HER2-targeting therapies, breast cancer patients who are defined as IHC1+ and IHC2+/FISH–negative are over 50% of all the breast cancer patients (47) and there is no HER2-targeting therapy indicating any discernible benefit for them. DS-8201a has the potential to show a clinical response toward the IHC1+ and IHC2+/FISH–negative populations as well.

In the PDX model, DS-8201a showed potent antitumor activity against T-DM1 primary insensitive cancer. MDR1 (p-glycoprotein) mediated efflux is known as one of the mechanisms having less sensitivity to tubulin polymerization and depolymerization inhibitors in the market, such as vincristine and paclitaxel, respectively (48, 49). Similarly, it was reported that DM1 is a substrate for MDR1 (37) and an anti-EpCAM-SMCC-DM1, which utilizes the same linker-payload as T-DM1, is also ineffective against MDR1-expressing tumors (50). On the other hand, DX-8951f exhibits potent antitumor activity in several xenograft models regardless of MDR1-expression, including a vincristine-resistant cell (22) and we have preliminary data that DXd showed cytotoxicity against MDR1-expressing cells. From these facts, DS-8201a is supposed to be an MDR1 poor substrate and has the possibility to overcome the primary resistance to T-DM1.

According to a phase II trial of T-DM1 (TDM4558g), however, the primary resistance to T-DM1 may be relatively infrequent, indicating around 20% (51), and the major population of T-DM1 prior treated patients is considered to have an acquired resistance to T-DM1 (52). As one of the mechanisms of acquired resistance to T-DM1, a loss of sensitivity to DM1, and a downregulation of HER2 protein were reported on the basis of preclinical assessment (53, 54). In the assessment, the sensitivity to CTP-11 in trastuzumab–maytansinoid conjugate (similar to T-DM1)–resistant MDA-MB-361 cells did not change, whereas about 3- to 4-fold loss of sensitivity to DM1-SMe was observed (53). Therefore, we greatly expect that DS-8201a is effective against tumors with acquired resistance to T-DM1, unless HER2 completely disappears from the cell membrane. It is because DS-8201a could be effective against HER2-low tumors.

The mechanism of action of the payload is also known to affect the safety profile of ADCs. In a clinical setting, the major adverse events of T-DM1 are thrombocytopenia and peripheral neuropathy as typical toxicities of tubulin inhibitor–conjugated ADCs (10, 26, 51). A platelet decrease was observed in a monkey study with T-DM1 (25), which is associated with thrombocytopenia limiting the MTD of T-DM1 to 3.6 mg/kg every 3 weeks in the clinic (26). Irreversible axonal degeneration by T-DM1 was noted in monkeys as well (25), which was considered to be correlated with peripheral neuropathy in humans (26). A repeated dose of DS-8201a to monkeys induced no toxicities suggestive of the thrombocytopenia or peripheral neuropathy which were observed in the monkey studies with T-DM1. DS-8201a caused pulmonary toxicity in monkeys at $\geq$30 mg/kg (every 3 weeks for 3 doses), while it was not observed in rats (antigen–nonbinding species). Similarly, T-DM1 caused infiltration of mononuclear cells into the interstitium of the lung in cynomolgus monkeys at $\geq$10 mg/kg (every 3 weeks for 4 doses), which was not seen in rats (25). The evidence of HER2 protein expression on cell membranes of epithelial cells in the lung in humans (55), and the absence of the pulmonary findings in rats seems to suggest that the pulmonary effects of T-DM1 and DS-8201a may be mediated by HER2 expression in the lung.

The preclinical safety profile warranted clinical investigation, and the phase I dose escalation was initiated in August 2015 in Japan (Trial registration ID: NCT02564900). In the phase I dose expansion, the tolerability and efficacy against T-DM1 prior treated breast cancer patients, trastuzumab prior treated gastric cancer patients, and HER2 low–positive breast cancer patients will be assessed. The results stated in the current article support the view that DS-8201a can become an attractive and promising HER2-targeting ADC with the novel topoisomerase I inhibitor, which provides an additional treatment option to current HER2-targeting therapies; it is effective not only against breast cancer, but also many types of HER2-expressing cancers, including T-DM1–refractory and low HER2–expressing cancers, and exhibits a great efficacy in patients.

Disclosure of Potential Conflicts of Interest

No potential conflicts of interest were disclosed.

Authors' Contributions

Conception and design: Y. Ogitani, T. Aida
Development of methodology: Y. Ogitani, T. Aida
Acquisition of data (provided animals, acquired and managed patients, provided facilities, etc.): Y. Ogitani, K. Hagihara, J. Yamaguchi, C. Ishii, N. Harada, M. Soma, H. Okamoto, I. Hayakawa
Analysis and interpretation of data (e.g., statistical analysis, biostatistics, computational analysis): T. Hirai, Y. Ogitani, T. Aida, J. Yamaguchi, S. Arakawa, R. Atsumi
Writing, review, and/or revision of the manuscript: Y. Ogitani, T. Aida, K. Hagihara, J. Yamaguchi, M. Oitate, S. Arakawa, R. Atsumi, T. Nakada
Administrative, technical, or material support (i.e., reporting or organizing data, constructing databases): T. Hirai, R. Atsumi, T. Nakada
Study supervision: Y. Abe, T. Agatsuma

The costs of publication of this article were defrayed in part by the payment of page charges. This article must therefore be hereby marked *advertisement* in accordance with 18 U.S.C. Section 1734 solely to indicate this fact.

Received November 18, 2015; revised March 17, 2016; accepted March 20, 2016; published OnlineFirst March 29, 2016.

References

1. Coussens L, Yang-Feng TL, Liao YC, Chen E, Gray A, McGrath J, et al. Tyrosine kinase receptor with extensive homology to EGF receptor shares chromosomal location with neu oncogene. Science 1985;230:1132–9.

2. Yan M, Parker BA, Schwab R, Kurzrock R. HER2 aberrations in cancer: implications for therapy. Cancer Treat Rev 2014;40:770–80.
3. Yan M, Schwaederle M, Arguello D, Millis SZ, Gatalica Z, Kurzrock R. HER2 expression status in diverse cancers: review of results from 37,992 patients. Cancer Metastasis Rev 2015;34:157–64.
4. Slamon DJ, Clark GM, Wong SG, Levin WJ, Ullrich A, McGuire WL. Human breast cancer: correlation of relapse and survival with amplification of the HER-2/neu oncogene. Science 1987;235:177–82.
5. Slamon DJ, Godolphin W, Jones LA, Holt JA, Wong SG, Keith DE, et al. Studies of the HER-2/neu proto-oncogene in human breast and ovarian cancer. Science 1989;244:707–12.
6. Slamon DJ, Leyland-Jones B, Shak S, Fuchs H, Paton V, Bajamonde A, et al. Use of chemotherapy plus a monoclonal antibody against HER2 for metastatic breast cancer that overexpresses HER2. N Engl J Med 2001; 344:783–92.
7. Bang YJ, Van Cutsem E, Feyereislova A, Chung HC, Shen L, Sawaki A, et al. Trastuzumab in combination with chemotherapy versus chemotherapy alone for treatment of HER2-positive advanced gastric or gastro-oesophageal junction cancer (ToGA): a phase 3, open-label, randomised controlled trial. Lancet 2010;376:687–97.
8. Geyer CE, Forster J, Lindquist D, Chan S, Romieu CG, Pienkowski T, et al. Lapatinib plus capecitabine for HER2-positive advanced breast cancer. N Engl J Med 2006;355:2733–43.
9. Baselga J, Cortes J, Kim SB, Im SA, Hegg R, Im YH, et al. Pertuzumab plus trastuzumab plus docetaxel for metastatic breast cancer. N Engl J Med 2012;366:109–19.
10. Verma S, Miles D, Gianni L, Krop IE, Welslau M, Baselga J, et al. Trastuzumab emtansine for HER2-positive advanced breast cancer. N Engl J Med 2012;367:1783–91.
11. Lewis Phillips GD, Li G, Dugger DL, Crocker LM, Parsons KL, Mai E, et al. Targeting HER2-positive breast cancer with trastuzumab-DM1, an antibody-cytotoxic drug conjugate. Cancer Res 2008;68:9280–90.
12. de Claro RA, McGinn K, Kwitkowski V, Bullock J, Khandelwal A, Habtemariam B, et al. U.S. Food and Drug Administration approval summary: brentuximab vedotin for the treatment of relapsed Hodgkin lymphoma or relapsed systemic anaplastic large-cell lymphoma. Clin Cancer Res 2012;18:5845–9.
13. Hamilton GS. Antibody-drug conjugates for cancer therapy: The technological and regulatory challenges of developing drug-biologic hybrids. Biologicals 2015;43:318–32.
14. Hinrichs MJ, Dixit R. Antibody drug conjugates: nonclinical safety considerations. AAPS J 2015;17:1055–64.
15. Pommier Y. Topoisomerase I inhibitors: camptothecins and beyond. Nat Rev Cancer 2006;6:789–802.
16. Stintzing S. Management of colorectal cancer. F1000Prime Rep 2014; 6:108.
17. Sudo K, Yamada Y. Advancing pharmacological treatment options for advanced gastric cancer. Expert Opin Pharmacother 2015;16:2293–305.
18. Kim A, Ueda Y, Naka T, Enomoto T. Therapeutic strategies in epithelial ovarian cancer. J Exp Clin Cancer Res 2012;31:14.
19. Ku GY, Ilson DH. Chemotherapeutic options for gastroesophageal junction tumors. Semin Radiat Oncol 2013;23:24–30.
20. Kalemkerian GP. Advances in pharmacotherapy of small cell lung cancer. Expert Opin Pharmacother 2014;15:2385–96.
21. Cid-Arregui A, Juarez V. Perspectives in the treatment of pancreatic adenocarcinoma. World J Gastroenterol 2015;21:9297–316.
22. Kumazawa E, Jimbo T, Ochi Y, Tohgo A. Potent and broad antitumor effects of DX-8951f, a water-soluble camptothecin derivative, against various human tumors xenografted in nude mice. Cancer Chemother Pharmacol 1998;42:210–20.
23. Abou-Alfa GK, Letourneau R, Harker G, Modiano M, Hurwitz H, Tchekmedyian NS, et al. Randomized phase III study of exatecan and gemcitabine compared with gemcitabine alone in untreated advanced pancreatic cancer. J Clin Oncol 2006;24:4441–7.
24. Hamblett KJ, Senter PD, Chace DF, Sun MM, Lenox J, Cerveny CG, et al. Effects of drug loading on the antitumor activity of a monoclonal antibody drug conjugate. Clin Cancer Res 2004;10:7063–70.
25. Poon KA, Flagella K, Beyer J, Tibbitts J, Kaur S, Saad O, et al. Preclinical safety profile of trastuzumab emtansine (T-DM1): mechanism of action of its cytotoxic component retained with improved tolerability. Toxicol Appl Pharmacol 2013;273:298–313.
26. Krop IE, Beeram M, Modi S, Jones SF, Holden SN, Yu W, et al. Phase I study of trastuzumab-DM1, an HER2 antibody-drug conjugate, given every 3 weeks to patients with HER2-positive metastatic breast cancer. J Clin Oncol 2010;28:2698–704.
27. Nakada T, Masuda T, Naito H, Yoshida M, Ashida S, Morita K, et al. Novel antibody-drug conjugates containing exatecan derivative-based cytotoxic payloads. Bioorg Med Chem Lett 2016;26:1542–5.
28. Widdison WC, Wilhelm SD, Cavanagh EE, Whiteman KR, Leece BA, Kovtun Y, et al. Semisynthetic maytansine analogues for the targeted treatment of cancer. J Med Chem 2006;49:4392–408.
29. Kawato Y, Aonuma M, Hirota Y, Kuga H, Sato K. Intracellular roles of SN-38, a metabolite of the camptothecin derivative CPT-11, in the antitumor effect of CPT-11. Cancer Res 1991;51:4187–91.
30. Shiose Y, Ochi Y, Kuga H, Yamashita F, Hashida M. Relationship between drug release of DE-310, macromolecular prodrug of DX-8951f, and cathepsins activity in several tumors. Biol Pharm Bull 2007;30:2365–70.
31. Niedergethmann M, Wostbrock B, Sturm JW, Willeke F, Post S, Hildenbrand R. Prognostic impact of cysteine proteases cathepsin B and cathepsin L in pancreatic adenocarcinoma. Pancreas 2004;29:204–11.
32. Aggarwal N, Sloane BF. Cathepsin B: multiple roles in cancer. Proteomics Clin Appl 2014;8:427–37.
33. Ruan J, Zheng H, Fu W, Zhao P, Su N, Luo R. Increased expression of cathepsin L: a novel independent prognostic marker of worse outcome in hepatocellular carcinoma patients. PLoS One 2014;9:e112136.
34. Zhang W, Wang S, Wang Q, Yang Z, Pan Z, Li L. Overexpression of cysteine cathepsin L is a marker of invasion and metastasis in ovarian cancer. Oncol Rep 2014;31:1334–42.
35. Francisco JA, Cerveny CG, Meyer DL, Mixan BJ, Klussman K, Chace DF, et al. cAC10-vcMMAE, an anti-CD30-monomethyl auristatin E conjugate with potent and selective antitumor activity. Blood 2003;102: 1458–65.
36. DiJoseph JF, Khandke K, Dougher MM, Evans DY, Armellino DC, Hamann PR, et al. CMC-544 (inotuzumab ozogamicin): A CD22-targeted immunoconjugate of calicheamicin. Hematol Meeting Rep 2008;5:74–7.
37. U.S. Food and Drug Administration. Kadclya biologic license application (125427Orig1s000). Pharmacol Rev 2013.
38. Lewis GD, Figari I, Fendly B, Wong WL, Carter P, Gorman C, et al. Differential responses of human tumor cell lines to anti-p185HER2 monoclonal antibodies. Cancer Immunol Immunother 1993;37:255–63.
39. Clynes RA, Towers TL, Presta LG, Ravetch JV. Inhibitory Fc receptors modulate in vivo cytotoxicity against tumor targets. Nat Med 2000;6: 443–6.
40. Yakes FM, Chinratanalab W, Ritter CA, King W, Seelig S, Arteaga CL. Herceptin-induced inhibition of phosphatidylinositol-3 kinase and Akt Is required for antibody-mediated effects on p27, cyclin D1, and antitumor action. Cancer Res 2002;62:4132–41.
41. Junttila TT, Akita RW, Parsons K, Fields C, Lewis Phillips GD, Friedman LS, et al. Ligand-independent HER2/HER3/PI3K complex is disrupted by trastuzumab and is effectively inhibited by the PI3K inhibitor GDC-0941. Cancer Cell 2009;15:429–40.
42. Xiao Z, Chen Z, Gunasekera AH, Sowin TJ, Rosenberg SH, Fesik S, et al. Chk1 mediates S and G2 arrests through Cdc25A degradation in response to DNA-damaging agents. J Biol Chem 2003;278:21767–73.
43. Furuta T, Takemura H, Liao ZY, Aune GJ, Redon C, Sedelnikova OA, et al. Phosphorylation of histone H2AX and activation of Mre11, Rad50, and Nbs1 in response to replication-dependent DNA double-strand breaks induced by mammalian DNA topoisomerase I cleavage complexes. J Biol Chem 2003;278:20303–12.
44. Kaufmann SH, Desnoyers S, Ottaviano Y, Davidson NE, Poirier GG. Specific proteolytic cleavage of poly(ADP-ribose) polymerase: an early marker of chemotherapy-induced apoptosis. Cancer Res 1993;53: 3976–85.
45. Wolff AC, Hammond ME, Hicks DG, Dowsett M, McShane LM, Allison KH, et al. Recommendations for human epidermal growth factor receptor 2 testing in breast cancer: American Society of Clinical Oncology/College of American Pathologists clinical practice guideline update. Arch Pathol Lab Med 2014;138:241–56.
46. Junttila TT, Li G, Parsons K, Phillips GL, Sliwkowski MX. Trastuzumab-DM1 (T-DM1) retains all the mechanisms of action of trastuzumab and efficiently inhibits growth of lapatinib insensitive breast cancer. Breast Cancer Res Treat 2011;128:347–56.

47. Schalper KA, Kumar S, Hui P, Rimm DL, Gershkovich P. A retrospective population-based comparison of HER2 immunohistochemistry and fluorescence in situ hybridization in breast carcinomas: impact of 2007 American Society of Clinical Oncology/College of American Pathologists criteria. Arch Pathol Lab Med 2014;138:213–9.
48. Fojo T, Menefee M. Mechanisms of multidrug resistance: the potential role of microtubule-stabilizing agents. Ann Oncol 2007;18Suppl 5:v3–8.
49. Takara K, Sakaeda T, Okumura K. An update on overcoming MDR1-mediated multidrug resistance in cancer chemotherapy. Curr Pharm Des 2006;12:273–86.
50. Kovtun YV, Audette CA, Mayo MF, Jones GE, Doherty H, Maloney EK, et al. Antibody-maytansinoid conjugates designed to bypass multidrug resistance. Cancer Res 2010;70:2528–37.
51. Burris HAIII, Rugo HS, Vukelja SJ, Vogel CL, Borson RA, Limentani S, et al. Phase II study of the antibody drug conjugate trastuzumab-DM1 for the treatment of human epidermal growth factor receptor 2 (HER2)-positive breast cancer after prior HER2-directed therapy. J Clin Oncol 2011;29:398–405.
52. Barok M, Joensuu H, Isola J. Trastuzumab emtansine: mechanisms of action and drug resistance. Breast Cancer Res 2014;16:209.
53. Loganzo F, Tan X, Sung M, Jin G, Myers JS, Melamud E, et al. Tumor cells chronically treated with a trastuzumab-maytansinoid antibody-drug conjugate develop varied resistance mechanisms but respond to alternate treatments. Mol Cancer Ther 2015;14:952–63.
54. Li G, Fields C, Parsons K, Guo J, Phillips GL. Trastuzumab-DM1: mechanisms of action and mechanisms of resistance. 101st AACR Annual Meeting: 2010 April 17–21, 2010, Washington, DC; Abstract No. 223.
55. Press MF, Cordon-Cardo C, Slamon DJ. Expression of the HER-2/neu proto-oncogene in normal human adult and fetal tissues. Oncogene 1990; 5:953–62.